RESEARCH ARTICLE

Macromolecular Chemistry and Physics
www.mcp-journal.de

Adaptable Polyurethane Networks Containing Tertiary Amines as Intrinsic Bond Exchange Catalyst

*Lars Schwarzer and Seema Agarwal**

Vitrimers exhibit unique properties, such as thermal recyclability akin to thermoplastics, while structurally mirroring thermosets in terms of strength, durability, and chemical resistance. However, a significant limitation of these materials is their dependence on an external catalyst. Consequently, this research aims to develop vitrimer materials that incorporate an intrinsic catalyst, thus maintaining excellent thermomechanical properties and recyclability. Polyaddition polymerization is employed to synthesize the desired polymer, incorporating a self-synthesized tertiary amine unit, (bis(2-hydroxyethyl)-3,3′-((2-(dimethylamino)ethyl)azanediyl)dipropanoate) (*N*-diol), as an internal catalyst for transcarbamoylation and potential transesterification reactions. The resulting polymer, with a gel content of 97% and a glass transition temperature of 29 °C, is fabricated into test samples for comprehensive thermal and mechanical evaluations. The material demonstrates an initial Young's modulus of 555 MPa, retaining 81% of this value after two recycling processes. Additionally, using stress relaxation analysis (SRA), a topology freezing temperature of 82 °C, indicative of the characteristic Arrhenius-like relaxation behavior, is identified with a bond exchange activation energy of 163 kJ mol^{-1}.

1. Introduction

In 2011, French physicist Ludwik Leibler pioneered a novel category of polymer materials, merging the advantageous qualities of both thermosets and thermoplastics, starting with epoxy-based polyester resins.[1,2] These materials, known as vitrimers, are characterized by their high cross-link density and complete insolubility in water and organic solvents at all temperatures, akin to thermosets. However, vitrimers stand apart with their unique attributes, including self-healing properties and the capability to be welded and reshaped, reminiscent of thermoplastics.[3–7] The defining behavior of vitrimers is attributed to the presence of interchangeable chemical bonds also known as covalent adaptable networks (CANs), allowing for bond exchange reactions.[8] These reactions exhibit an Arrhenius-like temperature dependence, which enables reprocessability while the cross-link density in vitrimers remains constant.[9] The reprocessability aspect of these chemically cross-linked materials is particularly promising for reuse and recyclability, aligning with the escalating focus on developing recyclable plastics amidst growing concerns about the occurrence of microplastics, plastic waste management, plastic pollution of land and seas, and the pursuit of a sustainable society including circular economy.[10–13] The reprocessing and recycling capabilities of vitrimers present a promising approach to address the challenge of recycling covalently cross-linked thermosets, which are currently difficult or impossible to recycle. By increasing the recyclability of polymers and products at the end of their lifecycle, we can significantly reduce the likelihood of them turning into microplastic waste.

To date, the most common bond exchange reactions in vitrimers include, among others, transesterification, transcarbamoylation, transamination, transalkylation, disulfide exchange, or boronic ester exchange.[14–18] The very first example of vitrimers by Leibler et al. used transesterification reaction to demonstrate vitrimer behavior.[2] At room temperature, the material behaves like a standard thermoset, but at higher temperatures (beyond the vitrimer temperature, T_v), it can be processed like thermoplastics by activating bond exchanges through acid, base, or metal catalysts.[1,19] However, issues such as catalyst toxicity, leaching, and degradation during use and processing have spurred research into new vitrimer materials that can be processed like thermoplastics without additional catalysts.

Building on the understanding that β-activated esters undergo nucleophilic substitution reactions under milder conditions than nonactivated esters, low-temperature (≈150 °C), catalyst-free vitrimers were prepared using β-activated ester diethylmalonate and poly(hydroxyethyl methacrylate) as precursors, with free hy-

L. Schwarzer
Macromolecular Chemistry II, Advanced Sustainable Polymers
University of Bayreuth
95440 Bayreuth, Germany
S. Agarwal
Macromolecular Chemistry II
Advanced Sustainable Polymers
Bavarian Polymer Institute
University of Bayreuth
95440 Bayreuth, Germany
E-mail: agarwal@uni-bayreuth.de

The ORCID identification number(s) for the author(s) of this article can be found under https://doi.org/10.1002/macp.202400072

DOI: 10.1002/macp.202400072

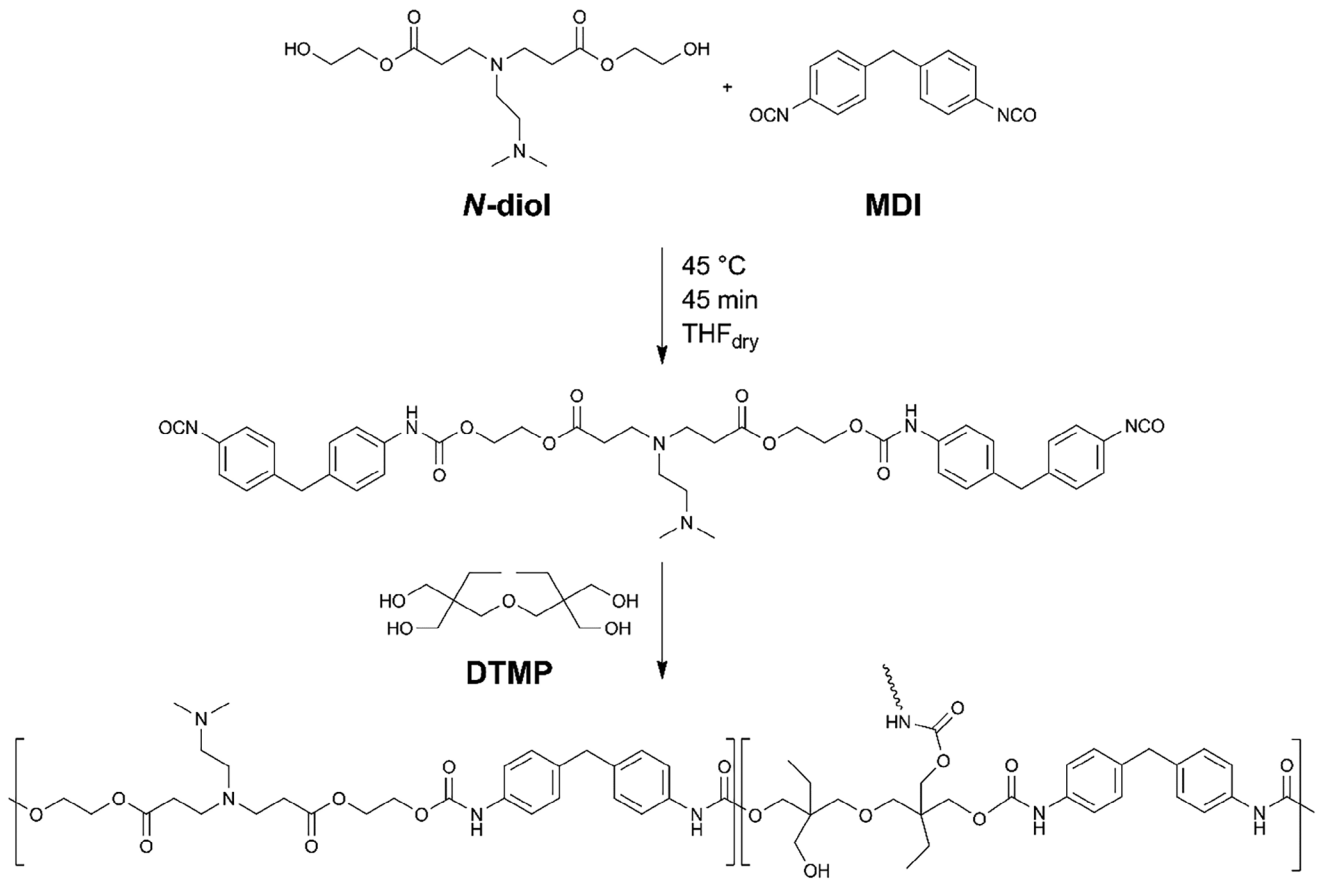

Scheme 1. Reaction scheme for the synthesis of cross-linked polymer by reaction of *N*-diol with MDI using DTMP as cross-linker.

droxyl groups for bond exchange reactions.[20] Another example of catalyst-free, heat- and pressure-processable vitrimers, based on carbamate exchange reactions, was reported by Dichtel and co-workers. These cross-linked polyurethanes, prepared by reacting bis(cyclic carbonate) and tris(2-aminoethyl)amine with free hydroxyl groups, exhibited stress relaxation under appropriate temperature and pressure conditions via transcarbamoylation reactions.[18] Further building on the idea of β-activated esters was done by Sumerlin et al. They used the commercially readily available vinyl monomers methyl methacrylate and (2-acetoacetoxy)ethyl methacrylate to first form a copolymer precursor containing malonate moieties in the side chains. These malonates were utilized in the formation of vinylogous urethanes through the reaction with excess tris(2-aminoethyl)amine yielding a thermally processable and recyclable material with free amines acting as catalyst.[21]

Our work focuses on synthesizing and characterizing polyurethane vitrimer materials processable without external catalysts. We designed the polymer structure to include a tertiary amine enhancing exchange reactions as an inherent part of the repeat unit structure. A self-made diol with a tertiary amine (the base catalyst) as a side-chain ((bis(2-hydroxyethyl)-3,3′-((2-(dimethylamino)ethyl)azanediyl)dipropanoate) (*N*-diol) was reacted with 4,4′-methylenediphenyldiisocyanate (MDI) and a cross-linker, di(trimethylolpropane) (DTMP), to prepare the polyurethane vitrimer. The quaternized linear polyurethanes based on *N*-diol are known from our previous work.[22] To modify mechanical properties, a copolyurethane vitrimer using additional diol-terminated poly(tetrahydrofuran) (PTHF–diol) was also prepared. The processability is evaluated by heat pressing. The thermal, structural, mechanical, and rheological properties of these polymers are determined using techniques like thermogravimetric analysis (TGA), dynamic mechanical thermal analysis (DMTA), rheology, solid-state NMR, Fourier-transform infrared spectroscopy (FTIR), and uniaxial tensile testing. Overall, this work aims to contribute to the development of more sustainable, safer vitrimers with advanced processability, and high-performance properties.

2. Results and Discussion

N-diol and MDI were reacted in the presence of the cross-linking agent DTMP to achieve the desired cross-linked polymer (**Scheme 1**). DTMP was chosen as the desired cross-linker due to its superior solubility in organic solvents in contrast to pentaerythritol. The resulting polymer is designated as NDPUV0. The cross-linking reaction ultimately leading to gelation was fast, resulting in complete gelation after approximately 40 min. The final polymer after workup was obtained in the form of white powder. The polymer was subjected to solvent extraction using THF. NDPUV0 exhibited a high gel content of 84% and a moderate solvent uptake of 150%, without prior solvent extraction. Due to

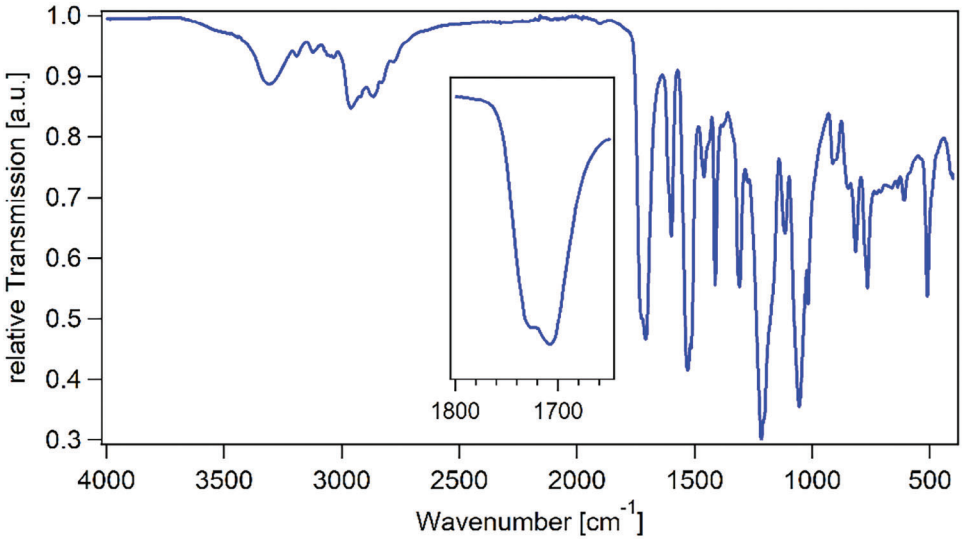

Figure 1. FTIR spectrum of NDPUV0.

the cross-linked nature of the polymer, the anticipated structure is verified by FTIR and solid-state NMR spectroscopy due to its insolubility.

The FTIR spectrum of neat NDPUV0 is depicted in **Figure 1**. The observed spectra align with the anticipated polymer structure. Notably, no free isocyanate (≈2270 cm^{-1}) is detected. The stretching vibrations of aromatic C—H (MDI) and aliphatic C—H (*N*-diol) are observed at 2940 and 2870 cm^{-1}, respectively. The stretching vibration of aromatic C=C bonds is visible at 1600 cm^{-1}. The N—H stretching vibrations of the urethane groups are observed at 3300 cm^{-1}. The corresponding carbonyl stretching vibrations are also evident, with highlighted peaks at 1730 and 1710 cm^{-1}. This splitting can be attributed to hydrogen bonding between the urethane N—H groups and both the carbonyl groups (C=O) of the MDI urethane and the *N*-diol ester groups. This hydrogen bonding weakens the carbonyl bonds which leads to an absorption shift to lower wavenumbers, resulting in hydrogen bonded and non-bonded carbonyls.

Additional qualitative structural analysis was carried out using solid-state NMR techniques, including ^{1}H, ^{13}C cross-polarization (CP), and ^{15}N CP-NMR spectroscopy. The collected data, as seen in Figure S1 (Supporting Information), confirm the anticipated structure. Additionally, tertiary amines, lacking attached protons, are not easily discernible in the nitrogen spectrum using cross-polarization experiments. Nevertheless, no unexpected signals were observed apart from these observations. The data align with the anticipated structure and are consistent with the findings from FTIR analysis.

The present network showed a glass transition temperature (T_g) of 76 °C as measured by DMTA (**Figure 2**). Vitrimers possess a distinctive glass transition temperature, the topology freezing temperature (T_v), which is characterized by their Arrhenius-like relaxation behavior. At T_v the polymer network will enter a flowable state, permitting topology alterations via bond exchange reactions. Conversely, below T_v, the network becomes immobilized, and the polymer chains are rendered incapable of motion. This temperature was defined by Leibler as at the point of the conventional liquid to solid transition viscosity (η) of 10^{12} Pa s.[9,23] T_v determination was done through calculations based on DMTA measurements, combined with relaxation times derived from stress relaxation analysis (SRA) as described through the Maxwell relation and Poisson's ratio. These DMTA temperature ramps are essential for determining both the glass transition temperature T_g and the value of the rubber plateau modulus $E'(T)$.

The rubber plateau storage modulus (E') was measured at 110 °C, because at higher temperatures the material starts degrading as seen by TGA experiments. From the obtained graphs, the plateau modulus $E'(T)$ was determined to be 1.5 MPa. The SRA data and resulting relaxation times at different temperatures were obtained through rheology experiments under constant strain conditions. The SRA data and the corresponding Arrhenius plot are shown in **Figure 3**A and B. The relaxation times exhibited a linear relationship under Arrhenius conditions,

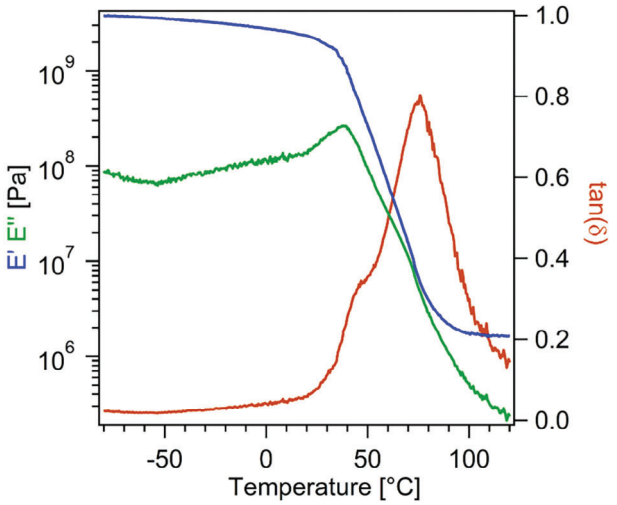

Figure 2. DMTA curves of NDPUV0 recorded at a heating rate of 2 K min^{-1} over a temperature range from −80 to 120 °C.

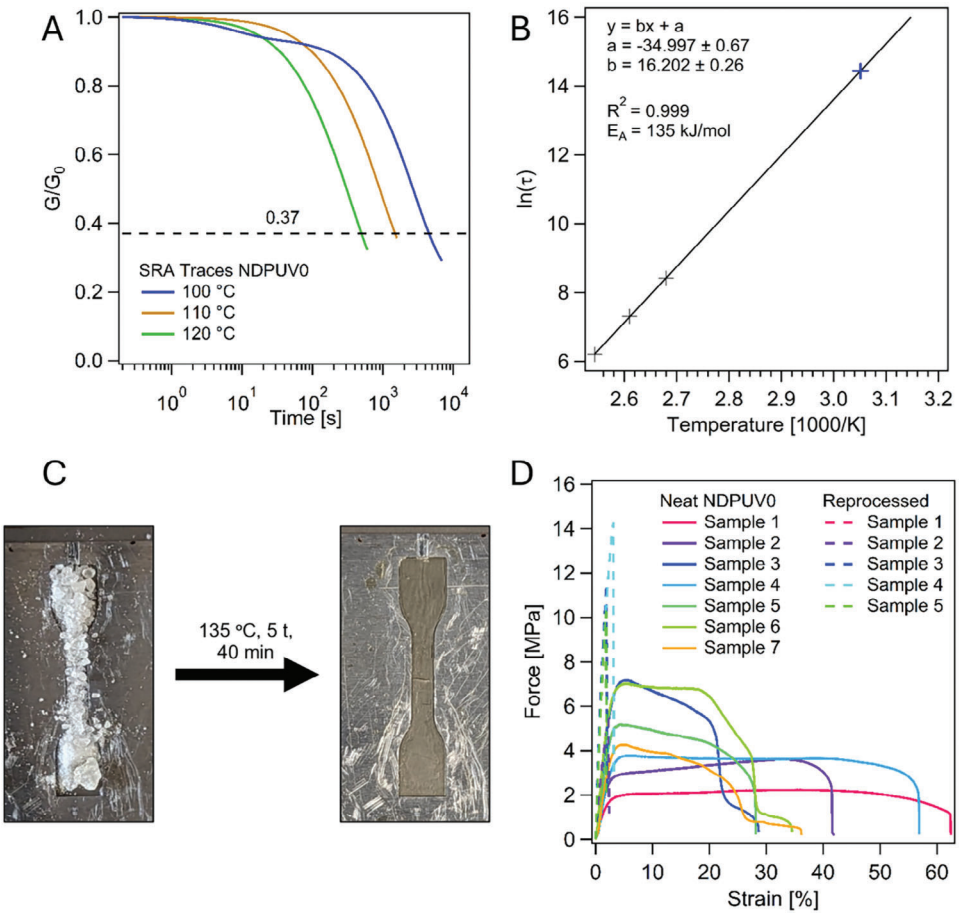

Figure 3. A) Normalized smoothed relaxation modulus of NDPUV0 at various temperatures. B) Arrhenius plot of NDPUV0 with linear fit and calculated relaxation time at the liquid-to-solid viscosity transition. The dashed line indicates a relaxation to e^{-1} of the initial G_0 value. C) Hot pressing of NDPUV0 at 135 °C for 40 min at 5 t pressure and cooling down to room temperature provided a transparent and uniform sample. D) Stress–strain curves of NDPUV0 as obtained from uniaxial tensile testing on neat and reprocessed dog-bone samples.

which indicates the vitrimeric properties facilitated by the CAN and corresponding bond exchange reactions. The good fit of the data further supports the vitrimeric behavior of the polymers. The relaxation times for the material at 100, 110, and 120 °C were recorded as 4500, 1480, and 497 s, respectively. A notable aspect of its relaxation behavior is the absence of an additional metal catalyst to exhibit Arrhenius relaxation behavior. The sample demonstrates the possibility of polyurethanes with *N*-diol as internal catalyst to relax through chemical exchange reactions, as evidenced by the consistent application of the Arrhenius law (Figure 3B). The calculated theoretical relaxation time at the liquid-to-solid transition viscosity is used to determine the corresponding value for T_v by plotting it on the Arrhenius plot. The *x*-axis value for T_v calculation is 3.05. Therefore, the topology freezing temperature is estimated to be 55 °C (see the Supporting Information (p. 2) for calculation procedure). The slope of the Arrhenius fit is used to calculate the activation energy E_A of the bond exchange reactions by multiplying it with the universal gas constant *R*. The calculation yields an activation energy of 135 kJ mol^{-1}. The value falls within the expected range for catalyzed transcarbamoylation, which typically requires around 100–130 kJ mol^{-1}.[24]

The next step is the thermal processing of cross-linked NDPUV0 and the determination of the optimum conditions. Therefore, a processing study was conducted, wherein various temperatures ranging from 95 to 145 °C and times of 20 and 40 min were tested under constant 5 t pressure. The most favorable outcome for neat NDPUV0 was obtained at a temperature of 135 °C and a pressing time of 40 min. Special molds were utilized to ensure uniform dog-bone-shaped samples (Figure 3C). The prepared dog-bone samples were used in uniaxial tensile testing for the determination of the mechanical properties. Broken samples were thermally processed again under the same conditions to investigate the recyclability of the vitrimer material, which was carried out successfully. Stress–strain curves of neat and recycled samples are displayed in Figure 3D and in Table S1 and Figure S2 (Supporting Information). The high elastic modulus of 250 MPa is attributed to the short-length repetition units, resulting in a rather stiff polymer. The tensile stress at break ranged from 2 to 7 MPa. The mechanical properties underwent significant changes upon recycling. The material became 2.5 times stiffer after recycling. This is evident from a steep increase in the Young modulus, an almost complete loss of elasticity, and doubling of the maximum measured stress.

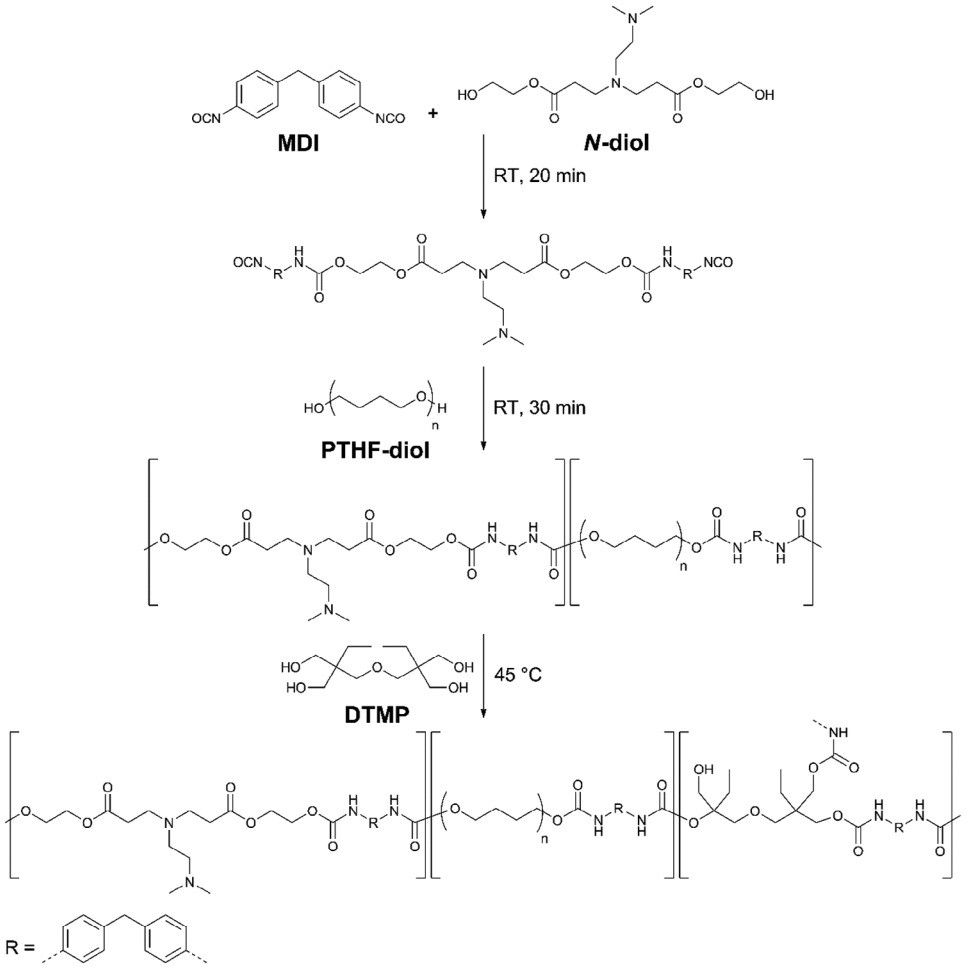

Scheme 2. Stepwise polymerization of CoPUV. First MDI and *N*-diol are allowed to react before PTHF is added as a chain extender which will further react with present MDI. During the last step, the cross-linker DTMP is added to ultimately form the desired polymer as a gel.

The next task was to prepare copolymer vitrimers by substituting a portion of *N*-diol with flexible PTHF–diol to improve both reprocessability and the mechanical properties. The synthesis of the vitrimer is conducted through a three-step, one-pot process. This involves the reaction of *N*-diol with MDI, followed by chain extension using PTHF–diol, and finally cross-linking with DTMP in the presence of trace amounts of Sn(II) catalyst to improve the reaction rate, as illustrated in **Scheme 2**. The Sn catalyst is removed from the polymer through thorough solvent extraction after gel formation. The polymers produced from this process are referred to as copolymer polyurethane vitrimers (*N*-diol PTHF copolymer vitrimer, CoPUVs). The formation of a bubble-free gel typically commences around 40 min after the addition of the catalyst during the cross-linking phase. The overall polymer formulation was chosen to still exhibit ≈1 mol% of unreacted OH-groups that could support bond exchange reactions as nonreacted nucleophile.

The polymer, once prepared, was subjected to extraction in THF at room temperature. Notably, the polymer demonstrated a high gel content of 97%, signifying a well cross-linked network structure. Additionally, it exhibited outstanding solvent absorption properties, with the capacity to absorb 241% of its initial weight. The polymer was obtained as a colorless material after drying, characterized by a soft rubbery texture, as shown in **Figure 4**.

The structure of the CoPUV was verified using FTIR and solid-state NMR techniques. The FTIR spectra of CoPUV are presented in **Figure 5**. Notably, no residual isocyanate was detected (≈2270 cm^{-1}). The stretching vibrations of aromatic C—H (MDI) and aliphatic C—H (*N*-diol) groups are observed at 2940 and 2870 cm^{-1}, respectively. The stretching vibration of aromatic C═C bonds appears at 1600 cm^{-1}. The N—H stretching vibrations of the urethane groups are evident at 3300 cm^{-1}, accompanied by corresponding carbonyl stretching vibrations with prominent peaks at 1730 and 1710 cm^{-1}. CoPUV also exhibits a carbonyl band splitting attributed to hydrogen bonding of the urethane groups. Solid-state NMR spectra (Figure S3, Supporting Information) primarily depict the PTHF segment of the polymer. However, the presence of incorporated MDI as a linking unit and urethane groups is also observable, as evidenced by the urethane ^{15}N peak at −278.1 ppm. The signals corresponding to the main *N*-diol monomer at around 50 ppm suggest its incorporation into

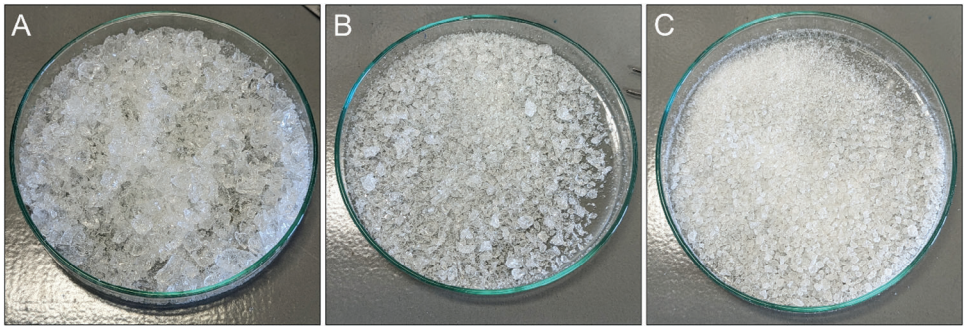

Figure 4. Polymer CoPUV A) after solvent extraction, B) after drying under room conditions for 24 h, and C) after crushing with dry ice.

the polymer. The DTMP cross-linker is predominantly identified through the carbon signal of the terminal CH_3 group, which can be observed at 8.1 ppm.

The T_g of CoPUV was determined to be ≈63 °C, as measured by DMTA and differential scanning calorimetry (DSC) (Figure S4, Supporting Information). TGA curves, obtained under both air and nitrogen atmospheres, exhibited remarkably similar trends. In both environments, a two-step degradation process was observed, beginning at an onset temperature of around 245 °C. At ≈400 °C, a second degradation step was noted, aligning with the typical behavior of polyurethanes. The overall degradation temperatures for CoPUV were found to be around 273 °C in an air atmosphere and 271 °C in nitrogen (Figure S5, Supporting Information).

The T_v was determined as described earlier, making use of both DMTA and SRA experiments. The DMTA data are depicted in **Figure 6**. The DMTA analysis of CoPUV reveals a prominent storage modulus plateau starting from 100 °C. The storage plateau modulus, determined at 150 °C, measures 2.79 MPa.

To investigate the relaxation behavior of the material, stress relaxation analysis was conducted using rheology under constant strain conditions. The resulting relaxation times at various temperatures were plotted alongside the corresponding Arrhenius plots, as depicted in **Figure 7**. The relaxation times display a linear relationship under Arrhenius conditions, demonstrating the vitrimeric relaxation characteristics up to a certain temperature. The relaxation times τ for the material were recorded as ≈1874 s at 130 °C, 455 s at 140 °C, 126 s at 150 °C, and 61 s at 160 °C. These

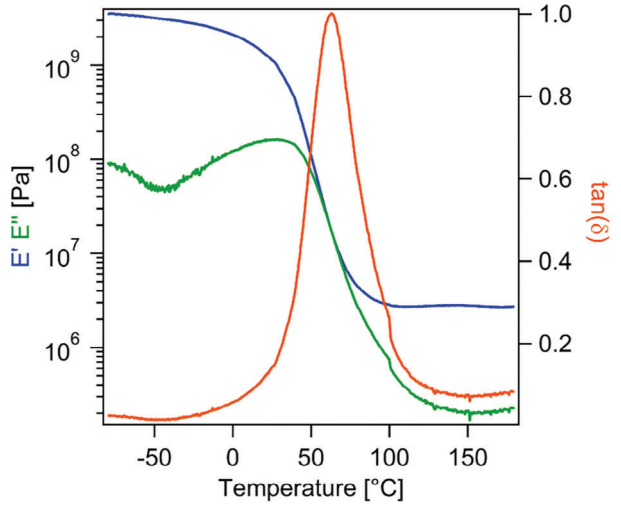

Figure 6. DMTA curves of CoPUV recorded at a heating rate of 2 K min^{-1} over a temperature range from −80 to 180 °C.

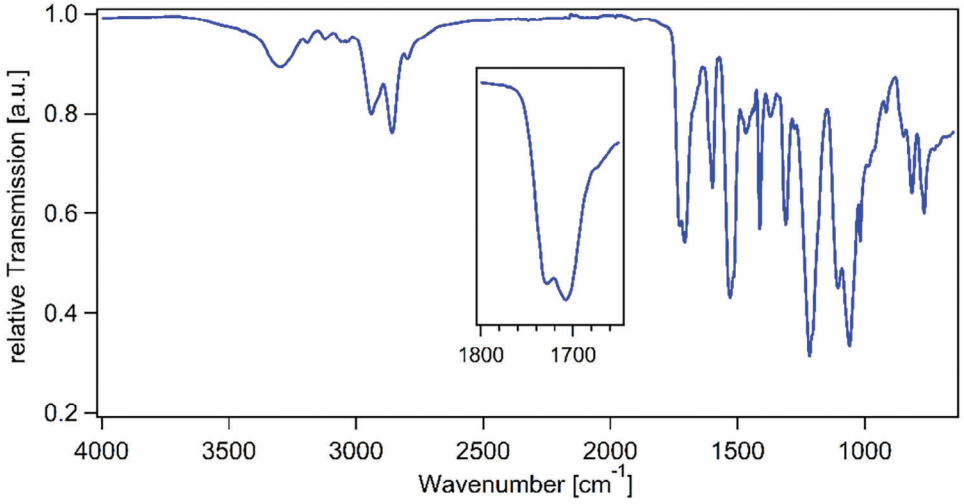

Figure 5. FTIR spectrum of CoPUV.

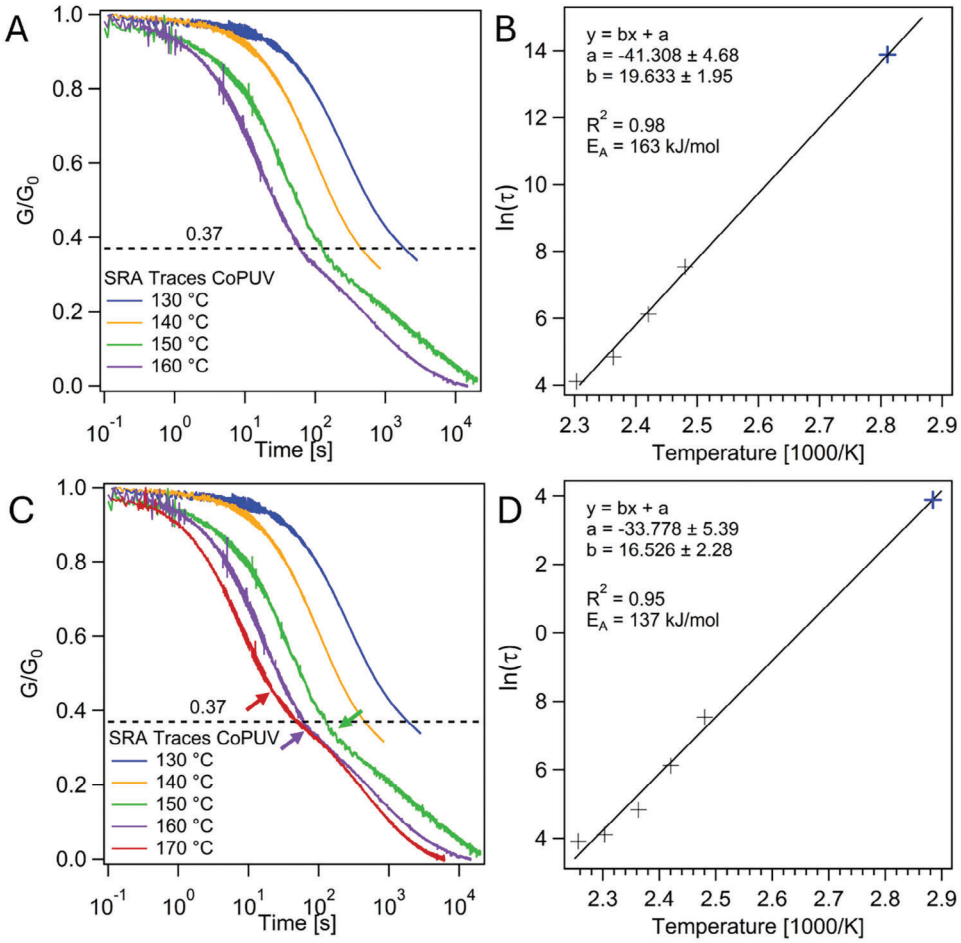

Figure 7. A) Normalized relaxation modulus of CoPUV at temperatures 130–160 °C. B) Corresponding Arrhenius plot of SRA curves with linear fit and calculated relaxation time at the liquid-to-solid viscosity transition. C) Normalized relaxation modulus of CoPUV at all measured temperatures including 170 °C and arrow indication of the observed kinks in the SRA curves. D) The resulting Arrhenius plot taking SRA at 170 °C into consideration. The dashed line indicates a relaxation to e^{-1} (37%) of the initial G_0 value.

times represent the duration needed for the relaxation modulus to reach 37% of its initial value and are obtained from Figure 7 at the intersection of the relaxation graphs with the dashed 0.37 line. The observed relaxation times indicate that the material can undergo relaxation within a moderately swift timeframe under the specified conditions and even achieve full relaxation (>99% of initial relaxation modulus *G*). However, full relaxation only occurs through a second relaxation step at high temperatures. This behavior becomes more pronounced at higher temperatures like 170 °C where the second relaxation step initiates after only 20 s (Figure 7C) and then follows the same relaxation trend as those observed at 150 and 160 °C. This may be due to the presence of an additional stress relaxation mechanism, such as transesterification, since the vitrimers in question have chemical structures featuring both ester and urethane functionalities, allowing for both types of dynamic exchange reactions. A visible change of functionality is also observable in FTIR measurements, where a shoulder appears in the carbonyl absorption band (Figure S6, Supporting Information) after the SRA experiments. The gel content after full relaxation was investigated through solvent extraction to see if this change happened due to the network collapsing and revealed that the material remained highly cross-linked, with a gel content of 98%.

The theoretical relaxation time τ^* at the liquid-to-solid transition viscosity, based on the Maxwell relation, was used in the Arrhenius plot to ascertain the corresponding values for the T_v of CoPUV. This value was determined to be 82 °C for CoPUV (see the Supporting Information (p. 2) for calculation procedure). Additionally, the activation energy for the bond exchange reactions in CoPUV was determined to be 163 kJ mol^{-1}, a high activation energy for transesterification reactions but a reasonable range for a potentially catalyzed transcarbamoylation reactions.[24,25] This confirms that the first stage of stress relaxation is likely due to transcarbamoylation. It is plausible that additional stress, such as pressure or other mechanical forces, might be necessary for the relaxation process to occur effectively. Another potential contributing factor could be the amount and the nature of the catalyst used in CoPUV. The use of a tertiary aliphatic amine as a catalyst, being a moderately strong base, could result in a higher activation barrier compared to a stronger organic base. This might explain the higher activation energy required for the bond exchange reactions in CoPUV.

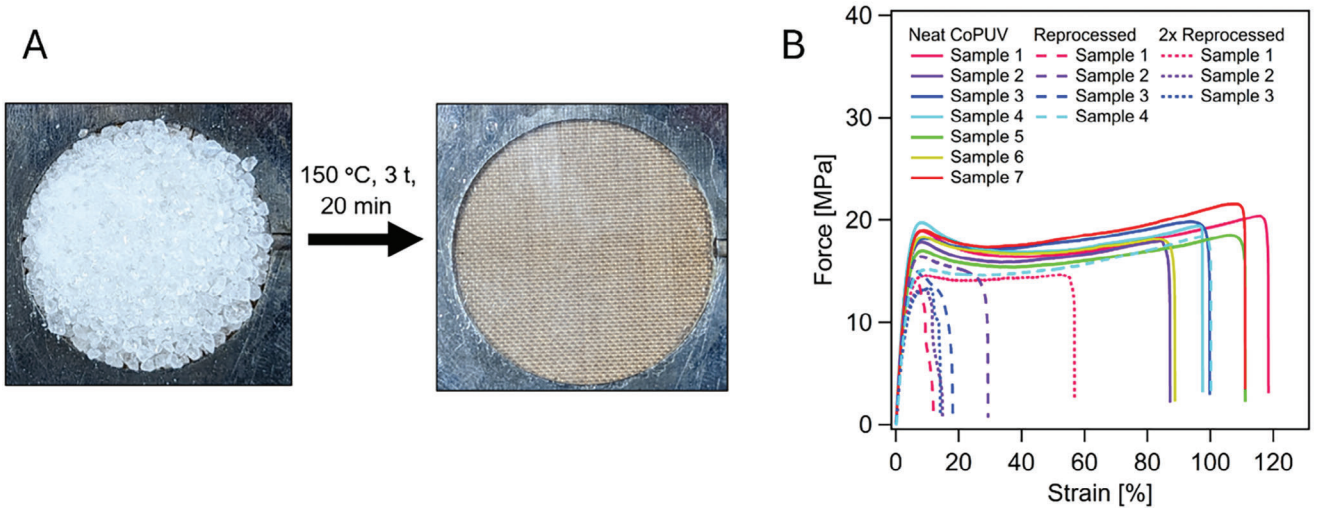

Figure 8. A) Neat CoPUV and processed CoPUV at 150 °C for 20 min at 3 t pressure. The sample thickness is 1 mm. The processed disk is transparent. The brown checked background is a thermally stable sheet used as a base for placing the mold in the heat press. B) Stress–strain curves of CoPUV as obtained from uniaxial tensile testing on neat and reprocessed dog-bone samples.

The plot of $\ln(\tau)$ versus temperature starts deviating from linearity on inclusion of stress relaxation data of 170 °C (Figure 7D) and the material no longer follows the Arrhenius law. It is unclear whether a second linear relation is applied or if the relation becomes nonlinear. Both the activation energy (163 kJ mol^{-1}) and T_V (82 °C) are therefore calculated excluding the datapoint for 170 °C. Future detailed studies should be carried out to thoroughly understand this mechanism and the reasons for this relaxation behavior.

The subsequent inquiry focused on the suitability of the prepared networks for thermal processing. To address this, a study was conducted to identify the appropriate processing conditions for CoPUV. A range of temperatures (from 130 to 150 °C) and durations (from 10 to 20 min) were experimented with, all under a constant pressure of 3 t. Under the optimized conditions, specifically, at 150 °C for 20 min and a pressure of 3 t, CoPUV could be successfully processed into films. These resultant films were colorless, clear, and homogeneous, displaying a smooth texture and being nonsticky to the touch. The processing of samples into molds of varying thicknesses was also feasible. Notably, the stress relaxation analysis experiments previously mentioned were conducted using polymer disks that were 1 mm thick. These disks were prepared through heat pressing, utilizing a round mold under the conditions described earlier (**Figure** 8A). This demonstrates the versatility of CoPUV being shaped into different forms and thicknesses, further highlighting its potential for various applications.

Utilizing the dog-bone sample mold, samples with a thickness of 0.5 mm were prepared specifically for tensile testing. These dog-bone-shaped samples were then subjected to uniaxial tensile testing to determine their mechanical properties. To investigate the recyclability of the vitrimer material, broken samples were recycled and processed again, with this cycle being repeated twice. The stress–strain curves of both the neat (original) and recycled CoPUV are displayed in Figure 8B (Figure S7, Supporting Information). This approach not only highlights the mechanical characteristics of CoPUV but also provides valuable insights into its potential for recycling and reuse, an important aspect in assessing the sustainability of such materials. Neat processed CoPUV shows a notable Young's modulus of 555 MPa while still maintaining a certain level of flexibility, allowing for up to 120% elongation. It is worth noting that CoPUV retains a substantial portion of its mechanical properties such as Young's modulus even after two reprocessing steps. The initial modulus of 555 MPa undergoes a reduction of only 8% after the first reprocessing and an additional 11% after the second reprocessing. The same trend applies to the maximum force at break. It decreases by ≈15% per reprocessing step, starting from ≈20 down to 14 MPa after two reprocessing steps. Although the strain at break shows on an average a decreasing trend after reprocessing cycles, a promising observation is that the reprocessed samples (sample 4 after one reprocessing and sample 1 of the neat, processed material; Figure 8B) still exhibit high strains, showcasing the potential of the material when well-recycled films are achieved. It should also be noted that the film quality varies a lot due to the limited amount of material and some samples showing edge defects. Nonetheless, the principle and potential of reprocessability of the cross-linked material could be shown. The mechanical data are summarized in Table S2 (Supporting Information). Optimization of the sample procedure preparation from an engineering point of view during recycling is required in the future, as well as the potential use of additives to improve processing stability and homogeneity. For second and subsequent recycling, no additional catalyst was added.

3. Conclusion

We presented a polyurethane-based covalent adaptable network containing tertiary amine moieties as internal catalyst for bond exchange reactions. The initial *N*-diol-based polymer already showed Arrhenius-like relaxation behavior, resulting from bond exchange reactions, and reprocessability. Upon reprocessing

the network became very brittle and stiff. Optimization of the polymer by tailoring the composition led to the final copolymer polyurethane vitrimer CoPUV. The incorporation of flexible PTHF–diol led to improved mechanical properties by doubling the Young modulus, increasing the gel content up to 92%, and improving reprocessability. Even after two reprocessing cycles, 81% of the initial Young modulus was retained. The crucial Arrhenius-like relaxation behavior was proven by SRA experiments and showed an exchange activation energy of 163 kJ mol^{-1}. Stress relaxation experiments hinted at an additional mechanism, such as transesterification, facilitated by the vitrimers' chemical structure, which includes both ester and urethane functionalities, permitting both types of dynamic exchange reactions. In conclusion, CoPUV can be a promising material for safer high-performance vitrimers without the need for an external catalyst, possessing good thermomechanical properties and reprocessability. Future studies should focus on understanding the mechanisms of stress relaxation and enhancing the reusability of the material through structural modifications.

4. Experimental Section

Materials: 2-Dimethylaminoethylamine (DMEA) was distilled before use. MDI (98%, Sigma–Aldrich), 2-hydroxyethylacrylate (HEA, >95%, TCI), DTMP (97%, Sigma Aldrich), and dimethyl sulfoxide (DMSO) (99.9%, Fisher Scientific GmbH) were used as received. PTHF (M_n = 1000 g mol^{-1}, Merck) was dried before use at 60 °C for 24 h at reduced pressure. THF (99.8%, Fisher Scientific GmbH) was run through a basic silica column (Brockmann I), desiccated over calcium hydride, and freshly distilled before use. Toluene (100%, VWR Chemicals) was dried over water-free calcium chloride, distilled, and stored over 3 Å molecular sieves. Tin(II) octoate (92.5 100%, Sigma–Aldrich) was used as a 2 M stock solution in dry toluene. Deuterated chloroform (99.8%, Deutero GmbH) was dried and stored over 3 Å molecular sieves.

Polymer Film and Sample Preparation: Films and dog-bone samples were prepared by heat pressing on a Carver 2518 hot press at varying temperature, pressure, and time, depending on the polymer. Dog-bone samples were prepared by filling a custom steel mold with polymer material tightly. It was placed between two steel plates and one sheet of nonstick Kapton foil on each side; a brass frame with the same height was also used to prevent any leakage of polymer into the press. After hot pressing, the films and samples were put into a water-cooled press where a pressure of 20–30 kN was applied to prevent any morphing during subsequent cooling. All molds should have an excess drain to obtain bubble-free and even samples. Dog-bone samples were pressed at a thickness of 0.5 mm and rheological samples at 1 mm. Films for processing testing were pressed at a thickness of 0.05 mm. Dog-bone geometry of the samples complied with DIN 53504 S3A.

Thermal Reprocessing: Reprocessing was also performed on the Carver 2518 hot press. Used samples in tensile testing were cut or ground into small pieces and filled into the dog-bone sample mold. The used conditions depended on the reprocessed polymer and were varied accordingly. After hot pressing, the samples were put into a water-cooled press where a pressure of 25 kN was applied to prevent morphing. Broken CoPUV samples were hot-pressed to 400 µm thin films instead and punched out using a hydraulic sample press by Coesfeld according to sample geometry DIN53504 S3A.

Gel Content and Swelling: The soluble portion of the polymer was calculated using a straightforward solvent extraction technique at room temperature. A rectangular section of the processed polymer film, measuring ≈ 0.5 cm × 0.5 cm × 0.5 mm, was immersed in 15 mL of THF and subjected to gentle agitation for a duration of 24 h. The weights of the film in its initial, swollen, and dried states (m_i, m_s, and m_d, respectively) were recorded. Subsequently, utilizing the following equations, the soluble fraction (sF) and swelling ratio (sR) were determined

$$sF = \frac{m_i - m_d}{m_i} \quad (1)$$

$$sR = \frac{m_s - m_i}{m_i} \quad (2)$$

Analytical Methods: Structural features were measured on a PerkinElmer Spectrum Two attenuated total reflection (ATR FTIR) spectrometer. The measurements were conducted in the mid-infrared region, 450–4000 cm^{-1}, with a resolution of 4 cm^{-1}, and a total of four scans were acquired to improve the signal-to-noise ratio. The measurements were performed at room temperature. To conduct further analysis of the polymer structure, solid-state NMR was employed. The experiments were carried out using a Bruker 400 MHz MAS NMR with 3.2 mm probes. ^{1}H and ^{13}C experiments were conducted at a spinning frequency of 12.5 kHz, while ^{15}N experiments were conducted at 10 kHz. Cross-polarization technique was utilized for ^{13}C and ^{15}N experiments. The ^{13}C and ^{1}H-NMR spectra were indirectly referenced with adamantane in relation to tetramethylsilane, while the ^{15}N-NMR spectra were directly referenced with glycine in relation to nitromethane. Solution state ^{1}H and ^{13}C NMR spectra were obtained on a Bruker Ultrashield 300 at room temperature and at 300 and 75 MHz, respectively. Approximately 10 mg of the sample was dissolved in 0.8 mL of dry $CDCl_3$.

Thermogravimetric Analysis: TGA was carried out using a Netzsch TG 209 F1 Libra machine under both air and nitrogen atmospheres. The samples were heated from 25 to 600 °C at a rate of 10 K min^{-1} in pierced lid 40 µL aluminum crucibles. A constant gas flow of 50 mL min^{-1} of nitrogen 5.3 and synthetic air (obtained from Rießner-Gase GmbH) was maintained during the entire duration of the analysis. Approximately 5–10 mg polymer was used per measurement.

Dynamic Mechanical Thermal Analysis: Temperature ramps were measured on a Rheometric Scientific DMTA IV instrument in tension film mode. The axial pre-force was determined through an initial strain sweep. The temperature ranges were varied depending on the polymer sample. A constant heating rate of 2 K min^{-1} and an angular frequency of 6.28 rad s^{-1} were used. An oscillating logarithmic strain increase from 0.01% to 0.05% was applied to guarantee sufficient strain on the samples throughout the measurement. The glass transition temperature was obtained from the maximum of the loss modulus. Samples were cut from dog-bone samples. The glass transition temperature obtained from the maximum in the loss factor tan(δ) describes the temperature with the highest viscous response, whereas the maximum in loss modulus corresponds to molecular motion. The T_g was obtained from the loss factor.[26]

Stress Relaxation Analysis: For the SRA experiments, an Anton Paar MCR 302 rheometer was used along with a P-TD 200 Peltier plate and an H-PTD 200 Peltier hood for temperatures below 200 °C. A plate–plate setup was used for 12 mm circular samples at 1 mm thickness. The 12 mm diameter samples were punched out from a 1 mm thick circular pressed sample. Prior to the stress relaxation experiments a strain sweep was performed at the corresponding temperature to ensure the range of the linear regime. The measured range reached from 0.01% to 5% strain. The experiments were performed at constant strain with a constant applied force of 1 N to guarantee good contact to the measuring axis. The used temperatures and applied strains depend on the polymer material. Each sample was allowed to equilibrate and relax for at least 10 min at the given temperature and in between measurements at different temperatures. Stress decay was monitored until 37% of the initial relaxation modulus was reached, and in the case of 150 and 160 °C of CoPUV, the material was fully relaxed (>99%). The curves were normalized to the initial maximum stress.

Uniaxial Tensile Testing: Uniaxial tensile testing was done on both neat and recycled samples in the afore mentioned dog-bone geometry, in accordance with DIN 53504 S3A, on a Zwick Roell Z0.5 tensile tester (BT1 FR 0.5TN-D14) with a 500 N KAF-TC force sensor. A standard measurement speed of 10 mm min^{-1} was used at varying preloads (0.06–0.1 cN) at a grip-to-grip separation of 20 mm at room temperature. The samples were

allowed to equilibrate under measuring room conditions for at least 48 h. Before each measurement, the thickness of each sample was obtained by calculating the mean value from three points along the gauge area. Length and width of the sample were fixed at 16 and 4 mm, respectively. The elastic modulus was determined automatically from the slope of the linear region of the stress–strain curves. At least three measurements per sample were taken.

Synthesis of N-Diol: 32.6 mL HEA (310 mmol, 36 g, 1.106 g mL^{-1}) was added to a three-necked round bottom flask along 30 mL dried THF. Over the course of 45 min, 16.9 mL DMEA (155 mmol, 13.7 g, 0.807 g mL^{-1}) was added dropwise using an addition funnel at room temperature. The reaction was heated to 45 °C after complete addition and was stirred for 24 h. Excess solvent was removed by distillation. Following preparation, the product was extracted eight times in 60 mL diethyl ether. Alternatively, the monomer could also be obtained in good purity by evaporating excess solvent without further extraction. The monomer was obtained as a sticky slightly yellow viscous liquid in 90% yield. ^{1}H-NMR (300 MHz, $CDCl_3$): δ = 4.24–4.17 (*m*, 4H, O—CH_2—CH_2—OH), 3.75–3.65 (*m*, 4H, O—CH_2—CH_2—OH), 2.76 (*t*, *J* = 6 Hz, 4H, N—CH_2—CH_2—CO), 2.54 (*t*, *J* = 6 Hz, 2H, N—CH_2—CH_2—N), 2.46 (*t*, *J* = 6 Hz, 4H, N—CH_2—CH_2—CO), 2.36 (*t*, *J* = 6 Hz, 2H, N—CH_2—CH_2—N), 2.19 (*s*, 6H, N—CH_3) ppm. ^{13}C-NMR (75 MHz, $CDCl_3$): δ = 173.0 (C═O), 66.3 (CH_2—OH), 60.6 (O—CH_2), 57.1 ((CH_3)$_2$—N—CH_2), 52.0 ((CH_3)$_2$—N—CH_2—CH_2—N), 50.2 (N—CH_2—CH_2—CO), 45.9 (CH_3), 33.1 (CH_2—CO) ppm.

Preparation of NDPUVs: 2.83 g of *N*-diol (8.82 mmol, 26 mol%) was dissolved in 60 mL dry THF in a thoroughly dried round bottom flask under Ar. Then 4.92 g of MDI (19.14 mmol) was added and stirred for 30 min at room temperature. 1.49 g of DTMP (5.94 mmol) was added and dissolved at 45 °C water bath temperature. The reaction was driven to completion until gel formation. The gel was then cut into small pieces allowing to dry under room conditions for 3 days in a Teflon dish. Further drying was done for 24 h at 60 °C *in vacuo*. The dried polymer was further crushed by an electrical mixer together with dry ice to obtain smaller and more homogeneous polymer particles. The polymer was dried again at 60 °C at reduced pressure. NDPUV0 was obtained as a colorless powder in 95% yield.

Preparation of CoPUV: 8.44 g of MDI (33.7 mmol) was dissolved in 60 mL dry THF in a thoroughly dried round bottom flask under Ar. 1.99 g of *N*-diol (6.2 mmol, 10 mol%) was pre dissolved in 40 mL THF and slowly added to the MDI solution over the course of 25 min using an addition funnel. Afterward, dry PTHF (6.80 mmol) was dissolved in 40 mL THF and added over the course of 35 min using an addition funnel. 2.66 g of finely mortared DTMP (10.6 mmol) was added, and the reaction was heated on a 45 °C water bath. To enhance the reaction rate, one droplet of $Sn(Oct)_2$ was added after the complete dissolution of DTMP. Gelation took place after ≈40 min, indicating the completion of the reaction. The resultant gel was then cut into smaller pieces, and a volume of 100 mL dry toluene was introduced to extract any remaining unreacted monomers and the Sn catalyst. The mixture was allowed to stir at room temperature for 24 h. Excess solvent was removed, and the polymer was dried under room conditions for 48 h. Thorough drying was done for 24 h at 60 °C in vacuo. The dried polymer was crushed by an electrical mixer together with dry ice to obtain smaller and more homogeneous polymer particles. The polymer was dried again for 24 h at 60 °C *in vacuo*. The resulting CoPUV was obtained as colorless soft and rubbery polymer particles in 95% yield.

Supporting Information

Supporting Information is available from the Wiley Online Library or from the author.

Acknowledgements

The authors would like to thank the Bavarian Polymer Institute at the University of Bayreuth, Germany, for allowing the use of equipment in the "Small Scale Polymer Processing" and "Synthesis and Molecular Characterization" Keylabs. The authors would also like to thank Dr. Reiner Giesa for doing DMTA measurements on the provided samples. Additional thanks go to Beate Bojer of the chair of Inorganic Chemistry III of the University of Bayreuth, Germany, for providing the solid-state NMR measurements.

Open access funding enabled and organized by Projekt DEAL.

Conflict of Interest

The authors declare no conflict of interest.

Data Availability Statement

The data that support the findings of this study are available in the Supporting Information of this article.

Keywords

covalent adaptable networks, internal catalysis, polymer networks, polyurethanes, vitrimers

Received: March 12, 2024
Revised: May 25, 2024
Published online: June 12, 2024

[1] M. Capelot, D. Montarnal, F. Tournilhac, L. Leibler, *J. Am. Chem. Soc.* **2012**, *134*, 7664.
[2] D. Montarnal, M. Capelot, F. Tournilhac, L. Leibler, *Science* **2011**, *334*, 965.
[3] X. Yang, L. Guo, X. Xu, S. Shang, H. Liu, *Mater. Des.* **2020**, *186*, 108248.
[4] Y. Xu, S. Dai, L. Bi, J. Jiang, H. Zhang, Y. Chen, *Chem. Eng. J.* **2022**, *429*, 132518.
[5] J. Ma, L. E. Porath, M. F. Haque, S. Sett, K. F. Rabbi, S. Nam, N. Miljkovic, C. M. Evans, *Nat. Commun.* **2021**, *12*, 5210.
[6] H. Liu, H. Zhang, H. Wang, X. Huang, G. Huang, J. Wu, *Chem. Eng. J.* **2019**, *368*, 61.
[7] E. M. Eger, S. Agarwal, *ACS Appl. Polym. Mater.* **2023**, *5*, 5141.
[8] C. J. Kloxin, T. F. Scott, B. J. Adzima, C. N. Bowman, *Macromolecules* **2010**, *43*, 2643.
[9] M. Capelot, M. M. Unterlass, F. Tournilhac, L. Leibler, *ACS Macro Lett.* **2012**, *1*, 789.
[10] J. F. Patrick, M. J. Robb, N. R. Sottos, J. S. Moore, S. R. White, *Nature* **2016**, *540*, 363.
[11] Y. Zhu, C. Romain, C. K. Williams, *Nature* **2016**, *540*, 354.
[12] H. Ritchie, V. Samborska, M. Roser, *Our World in Data* **2023**.
[13] G. G. N. Thushari, J. D. M. Senevirathna, *Heliyon* **2020**, *6*, e04709.
[14] W. Denissen, G. Rivero, R. Nicolaÿ, L. Leibler, J. M. Winne, F. E. Du Prez, *Adv. Funct. Mater.* **2015**, *25*, 2451.
[15] C. Li, Y. Chen, Y. Zeng, Y. Wu, W. Liu, R. Qiu, *Eur. Polym. J.* **2022**, *162*, 110923.
[16] M. M. Obadia, B. P. Mudraboyina, A. Serghei, D. Montarnal, E. Drockenmuller, *J. Am. Chem. Soc.* **2015**, *137*, 6078.
[17] H. Si, L. Zhou, Y. Wu, L. Song, M. Kang, X. Zhao, M. Chen, *Composites, Part B* **2020**, *199*, 108278.
[18] D. J. Fortman, J. P. Brutman, C. J. Cramer, M. A. Hillmyer, W. R. Dichtel, *J. Am. Chem. Soc.* **2015**, *137*, 14019.
[19] J. P. Brutman, P. A. Delgado, M. A. Hillmyer, *ACS Macro Lett.* **2014**, *3*, 607.
[20] S. Debnath, S. Kaushal, U. Ojha, *ACS Appl. Polym. Mater.* **2020**, *2*, 1006.

[21] J. J. Lessard, L. F. Garcia, C. P. Easterling, M. B. Sims, K. C. Bentz, S. Arencibia, D. A. Savin, B. S. Sumerlin, *Macromolecules* **2019**, *52*, 2105.
[22] P. Hu, A. Greiner, S. Agarwal, *J. Polym. Sci., Part A: Polym. Chem.* **2019**, *57*, 752.
[23] C. A. Angell, *Science* **1995**, *267*, 1924.
[24] J. P. Brutman, D. J. Fortman, G. X. de Hoe, W. R. Dichtel, M. A. Hillmyer, *J. Phys. Chem. B* **2019**, *123*, 1432.
[25] H. Noureddini, D. Zhu, *J. Am. Oil Chem. Soc.* **1997**, *74*, 1457.
[26] K. Whitcomb, https://www.tainstruments.com/pdf/literature/RH100.pdf (accessed: April 2024).

